journal

J. Am. Ceram. Soc., 77 [5] 1329–39 (1994)

Interfacial Microstructure and Chemistry of SiC/BN Dual-Coated Nicalon-Fiber-Reinforced Glass-Ceramic Matrix Composites

Ellen Y. Sun* and Steven R. Nutt*,†

Division of Engineering, Brown University, Providence, Rhode Island 02912

John J. Brennan*

United Technologies Research Center, East Hartford, Connecticut 06108

Glass-ceramic composites with improved high-temperature mechanical properties have been produced by incorporating continuous SiC fibers into a barium magnesium aluminosilicate matrix. Control of the fiber/matrix interface was achieved by a dual-layer coating of SiC/BN(C) applied to the fibers by CVD. The weakly bonded interface resulted in composites with high fracture toughness and strength up to 1100°C, and the composite system was oxidatively stable during long-term exposure to air at high temperatures. Composites with different thermal and mechanical histories were studied, and interfaces were characterized using transmission electron microscopy (TEM), Auger electron spectroscopy, and fiber pushout tests. Observations of interfacial microstructure were correlated with the mechanical properties of the composite and with interface properties determined from fiber push-out tests.

I. Introduction

FIBER-REINFORCED glass-ceramic composites are prospective materials for high-temperature, lightweight, structural applications.[1,2] In recent years, research has been carried out to characterize the fiber/matrix interface and the relationship of the interfacial morphology, chemistry, and degree of bonding to the resultant composite mechanical properties and interface stability.[3,4] These studies have revealed that polymer-derived Si-C-O or Si-C-N-O fibers that contain excess carbon and oxygen over stoichiometric SiC, such as Nicalon, Tyranno, and Dow Corning's MPDZ (methylpolydisilazane), form a carbon-rich fiber/matrix interfacial layer when incorporated into glass-ceramic matrices at high temperatures. The carbon-rich layer is relatively weak and consequently imparts high fracture toughness to the composites by allowing crack deflection to occur along the fiber/matrix interface and load transfer to occur from matrix to fiber. In the case of fibers that do not form an *in situ* carbon-rich layer during composite processing, the fiber/matrix interfacial bonding is strong, resulting in brittle failure and low composite toughness.[5]

Unfortunately, glass-ceramic matrix composites typically exhibit embrittlement and loss of strength and toughness when exposed to high-temperature oxidizing environments for long periods of time, particularly when stress is also applied. This embrittlement apparently occurs when the fiber/matrix interface is exposed to oxygen, and it is conjectured that this can transpire in one of two ways. First, oxygen can diffuse to the interface via matrix microcracks and react with carbon in the interfacial layer. Second, oxygen can reach the carbon interfacial layer via "pipeline" diffusion that initiates from cut ends of fibers exposed at the composite surface.[5] When this happens, a glassy oxide layer forms on the exposed fiber surfaces which bonds the fibers tightly to the matrix, resulting in brittle composite behavior. Regardless of which oxidation mechanism is prevalent, it is important to control the fiber/matrix interface in these composites to achieve relatively weak interfacial bonding (for crack deflection) while maintaining oxidative stability at high temperatures. One approach to this problem involves the use of fiber coatings applied to the fibers prior to composite fabrication. Such coatings can be engineered to achieve the desired interface strength and to improve the oxidation resistance.

In this paper, we describe the results of recent efforts to control the interfacial microstructure in fiber-reinforced barium magnesium aluminosilicate matrix composites using SiC/BN coatings applied by CVD. The changes in interface structure and chemistry as a function of composite processing and thermal history are investigated. The primary objectives of the work described are to assess the effectiveness of experimental coating and to develop an understanding of interface phenomena controlling mechanical behavior of these composites. An additional purpose of the work is to provide a basis for microstructural design of composite interfaces that result in improved composite properties at high temperatures.

II. Background

During the past few years, several studies have reported the results of attempts to use fiber coatings as a means of controlling the fiber/matrix interfacial properties in ceramic composites.[6–9] While most studies have dealt with fibers that bonded too strongly to achieve tough composite behavior, some have attempted to replace the carbon-rich zone with a similar weakly bonded coating that also had improved oxidative stability. CVD coatings such as BN[6] and SiC on BN[9] were deposited on small-diameter fibers such as the SiC-based Nicalon fiber (Nippon Carbon Co.) and the Si-N-C based HPZ fiber (hydridopolysilazane, from Dow Corning Corp.). Incorporating these coated fibers into glass-ceramic matrices such as lithium aluminosilicate (LAS) and barium magnesium aluminosilicate (BMAS) resulted in strong and tough composites that were oxidatively stable at high temperatures.

Previous work on BN-coated fibers has shown that high tensile strengths can be obtained if the BN coating is (a) amorphous or partly turbostratic in nature, and (b) has a composition

D. Clarke—contributing editor

Manuscript No. 194366. Received July 21, 1993; approved December 4, 1993.
Presented in part at the 95th Annual Meeting of the American Ceramic Society, Cincinnati, OH, April 21, 1993 (Paper No. SII-83-93).
Supported by the Air Force Office of Scientific Research (Contract No. F49620-92-C-0001) and by the National Science Foundation (E.Y.S. and S.R.N.) through a Materials Research Group (Grant No. DMR-9002994).
*Member, American Ceramic Society.
†Current address: Department of Materials Science, University of Southern California, Los Angeles, California 90089–0241.

that is close to stoichiometric BN but contains excess carbon.[10,‡] It has also been found that outward diffusion of boron during composite fabrication can prevent complete crystallization of glass-ceramic matrices.[9] The residual boron-bearing glassy regions degrade the high-temperature strength of the composites.[9] In order to prevent boron diffusion, a thin SiC overcoat can be applied to the BN(C) coating as a diffusion barrier. This SiC layer inhibits boron diffusion into the matrix and matrix element diffusion into the BN(C) coating, resulting in composites with superior elevated temperature properties compared to BN(C)-coated Nicalon fiber composites. These preliminary studies indicated that BMAS matrix composites reinforced with dual-coated Nicalon fibers have significant potential as tough, thermally stable, structural ceramic composites for applications to ~1200°C. From this brief review, it is clear that development of such composites for use in engineering applications requires an understanding of the microstructure and chemistry of the interfacial region, and how these factors influence the interfacial bonding and mechanical behavior of the composites.

III. Experimental Procedure

(1) Material

The glass-ceramic matrix selected for the present study was barium magnesium aluminosilicate (BMAS), and the reinforcement was a Si-C-O Nicalon fiber with a dual SiC/BN(C) coating. The BN(C) coating was deposited on the fiber by chemical vapor deposition at a temperature of ~1000°C using a proprietary precursor chosen to give an approximate composition of 40 at.% B, 40 at.% N, and 20 at.% C. The BMAS matrix was formulated to yield the barium osumilite composition on crystallization ($BaMg_2Al_3(Si_9Al_3O_{30})$), following the procedures described in Ref. 11. Composite panels (100 mm × 100 mm) were fabricated by hot-pressing a layup of 0/90° plies at 1450°C for 5 min under 6.9 MPa pressure, resulting in fiber loadings of ~50 vol%. After hot pressing, the composite panels were cut into bars and heat-treated ("ceramed") in argon at 1200°C for 24 h in order to crystallize the BMAS matrix to the barium osumilite phase.

Composites with four different thermomechanical histories were produced. The conditions included the following: (1) as-pressed; (2) ceramed; (3) tensile stress-rupture-tested at 1100°C in air to a maximum stress of 165 MPa for a total time of over 344 h; and (4) thermally aged at 1200°C in air for 500 h.

(2) Mechanical Behavior

The mechanical properties of the composites were evaluated by flexural (three-point loading) and tensile testing at both room temperature and elevated temperature. Tensile stress-rupture experiments were conducted in air at 1100°C. In these experiments, an initial stress of 69 MPa was applied for 50 h. This stress was below the measured tensile proportional limit stress of 77 MPa. The stress was increased in 14-MPa increments, holding for 50 h at each stress level. The experiment was halted after ~350 h, having reached a stress of 165 MPa without fracture. Fiber indent testing was conducted using a nanoindenter to determine the debond energies and frictional sliding stresses of the fiber interfaces. Push-in experiments were conducted on polished composite sections ~3 mm thick, using a truncated diamond cone with a 10-μm flat and a 55° included angle. Experiments were conducted at a crosshead speed of 12.7 μm/min, and 8–18 fibers were tested from each sample.

(3) Microstructure Characterization

The interfacial microstructures of composites with the four thermomechanical histories were characterized using analytical and high-resolution transmission electron microscopy (HRTEM). Thin foils for TEM were prepared in a conventional manner by mechanical polishing, dimpling, and ion milling. Specimens were examined using a JEOL 2010 microscope fitted with a Noran X-ray spectrometer capable of light-element detection. Composition analysis of microstructural features was performed with energy dispersive spectroscopy (EDS) using probe sizes of 10 or 15 nm.

Composition depth profiles of the composite interfaces were obtained using scanning Auger electron microscopy (SAM). The composite samples were fractured outside of the SAM vacuum chamber in a direction parallel to the 0° fibers so that fiber surfaces and matrix troughs from which fibers had pulled away were exposed. An exposed fiber surface and an adjacent matrix trough were then depth-profiled in the spot mode by argon ion sputtering through the interfacial coatings and into the Nicalon fiber and the BMAS matrix, respectively.

IV. Results and Discussion

(1) Mechanical Properties

The flexural properties of the composite are summarized in Table I, where each number represents the average of 10 or more measurements, with the exception of the thermally aged material. The composite strength is excellent from room temperature to 1200°C, but declines by about 20% after thermal aging at 1200°C in air for 500 h. The typical stress–strain behavior of the composite is shown in Fig. 1 for test temperatures of 1100°, 1200°, and 1300°C. At 1100° and 1200°C, the strengths remain high, as do the elastic moduli (79 and 69 GPa, respectively). However, at 1300°C, the composite properties decline significantly, primarily because of matrix softening. The tensile strengths are approximately half of the flexural strengths at 1100° and 1200°C, and the stress–strain curves appear similar in shape to those shown in Fig. 1.

The results of fiber indentation (push-out) experiments are summarized in Table II. The data were analyzed using approaches described by Marshall[12] and by Marshall and Oliver.[13] The Marshall analysis (M) yields a value, τ, that corresponds to a frictional sliding stress (in MPa), while the Marshall and Oliver (M&O) analysis is an extension of the previous approach with an added bonding component (G), which is referred to as the debond energy (in J/m^2). The values obtained by these approaches were relatively high, indicating a strongly bonded interface. However, the data exhibited large scatter, a phenomenon that was attributed to variations in interfacial microstructure, to be discussed in the following section. After 500 h at 1200°C in air, the values of τ and G declined by ~20% and ~55%, respectively. This decline, together with the degradation of the flexural properties, can be related to changes in the interfacial microstructure as described below.

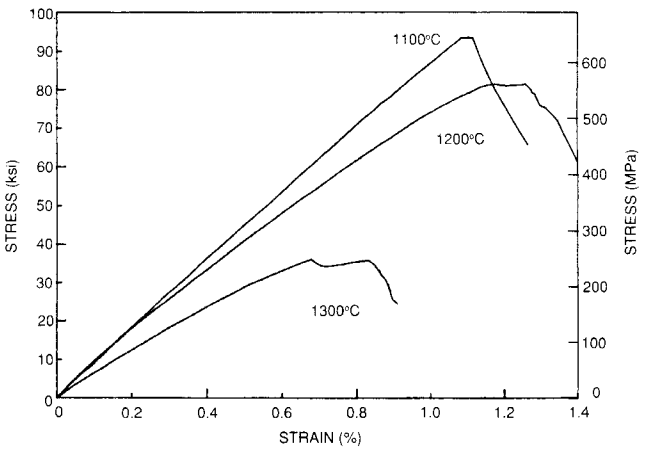

Fig. 1. Stress vs strain curve calculated from load–deflection measurements during high-temperature flexural deformation of BMAS matrix/SiC/BN/Nicalon fiber composite.

‡Carbon is reportedly added to BN coatings to prevent fiber strength degradation associated with application of the BN coating. Although it is uncertain exactly how the carbon enters the B-N-C structure in these coatings, a large degree of carbon substitution for nitrogen is reportedly possible in the turbostratic BN structure. This factor may have important implications with respect to the oxidation resistance of the coating relative to BN with free carbon.

Table I. Ultimate Strength (Three-Point Flexure) Properties of BMAS Matrix/SiC/BN/ Nicalon Fiber Composites

Room-temperature σ (MPa)				High-temperature σ (MPa)		
As-pressed	Ceramed	550°C, O_2, 100 h	1200°C, air, 500 h	1100°C	1200°C	1300°C
655	675	620	510	648	565	248

Table II. Results of Fiber Indentation (Push-out) Experiments of BMAS Matrix/SiC/BN/ Nicalon Fiber Composites

Heat treatment	σ (MPa)*	τ (MPa)		G(M&O) (J/m²)[‡]
		τ(M)[†]	τ(M&O)[‡]	
As-pressed	655	111 ± 48	101 ± 48	8.6 ± 9.8
Ceramed	675	139 ± 95	135 ± 72	7.2 ± 8.8
550°C, 100 h, O_2	620	144 ± 53	128 ± 47	8.6 ± 7.2
1200°C, 500 h, air	510	89 ± 56	90 ± 48	3.6 ± 5.2

*Room temperature. [†]Marshall. [‡]Marshall and Oliver.

(2) TEM Observations

(A) As-Pressed Composite: Features typical of the interface microstructure in an as-pressed composite are shown in Fig. 2. Appearing left to right in the figure are the Nicalon fiber, the BN(C) coating, and the SiC coating, together with corresponding inset diffraction patterns. As reported previously,[14,15] the fibers are microcrystalline and consist of randomly oriented β-SiC crystallites a few nanometers in size, with a small amount of amorphous phase. The selected area diffraction (SAD) pattern from the Nicalon fiber shows continuous diffuse rings indicative of extremely fine, randomly oriented grains. The BN(C) layer exhibits a turbostratic structure and is comprised of nano-scale crystallites. Previous work has indicated that similar BN(C) coatings are actually single-phase BN with a large degree of carbon substitution for nitrogen in the hexagonal BN lattice.[16] The BN(C) coating, henceforth referred to simply as BN, was often heterogeneous and was composed of several sublayers caused by the multiple passes through the reactor during chemical vapor deposition. Between the coating and the fiber is a subtle dual layer slightly rich in silica (dark) and carbon (light). (This feature is discussed below.) The SiC coating deposited onto the BN layer consisted of randomly oriented β-SiC crystallites, several hundred nanometers in diameter. Twins were evident inside the grains, which is typical of CVD SiC. As shown in the SAD pattern, the SiC coating produced strong diffraction spots arranged in discontinuous rings, indicating a polycrystalline structure with larger grains than the nanocrystalline Nicalon fiber.

Partial coarsening of the BN coating was often observed in the composite. Figure 2 shows that the BN adjacent to the SiC layer is coarse compared to the BN adjacent to the Nicalon fiber. The coarsening or crystallization of the turbostratic BN layer in this composite is associated with detachment of the SiC overlayer from the BN layer, which allows oxide glass from the matrix to penetrate and form a thin amorphous layer between the SiC and BN layer, as shown in Fig. 2. This assertion is supported by the scanning Auger depth profile in Fig. 3, which shows that matrix elements, primarily silicon, barium, and aluminum, have diffused into the BN layer. Figure 4 is a high-resolution image of the BN/SiC interfacial region, showing a ~20-nm film of glassy phase separating the SiC coating from the BN coating. The coarse BN exhibits wavy lattice fringes corresponding to the basal planes which tend to lie parallel to the glass film. The composition of the glass film, determined by EDS, was similar to that of the BMAS matrix, containing BaO, MgO, and Al_2O_3. Similar observations of turbostratic BN on oxide substrates were reported by Borek *et al.*,[17] who found that physical mixtures of a BN polymeric precursor with oxide particles such as MgO, Al_2O_3, and TiO_2 yielded crystalline, tightly adherent coatings of hexagonal BN on the oxide surfaces, with the BN (0001) basal planes aligned parallel to the surfaces. Despite detachment from the BN layer, the SiC overlayer

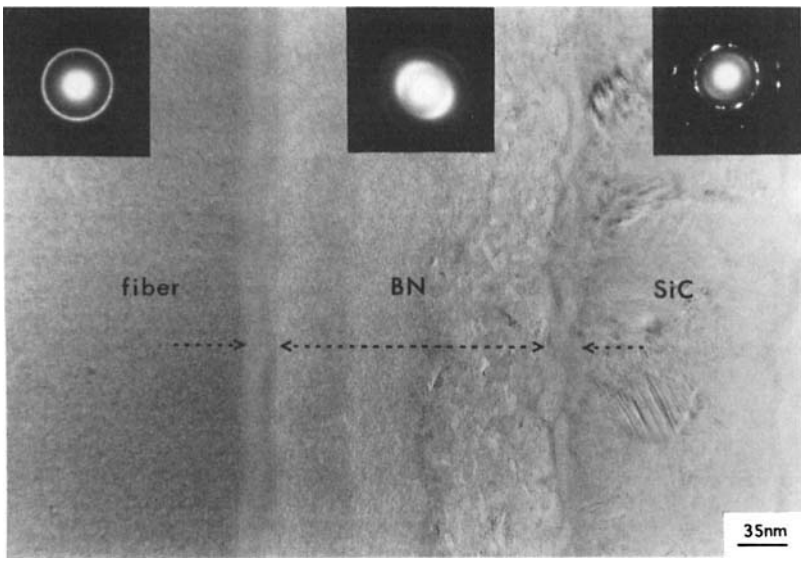

Fig. 2. Interfacial microstructure in as-pressed composite.

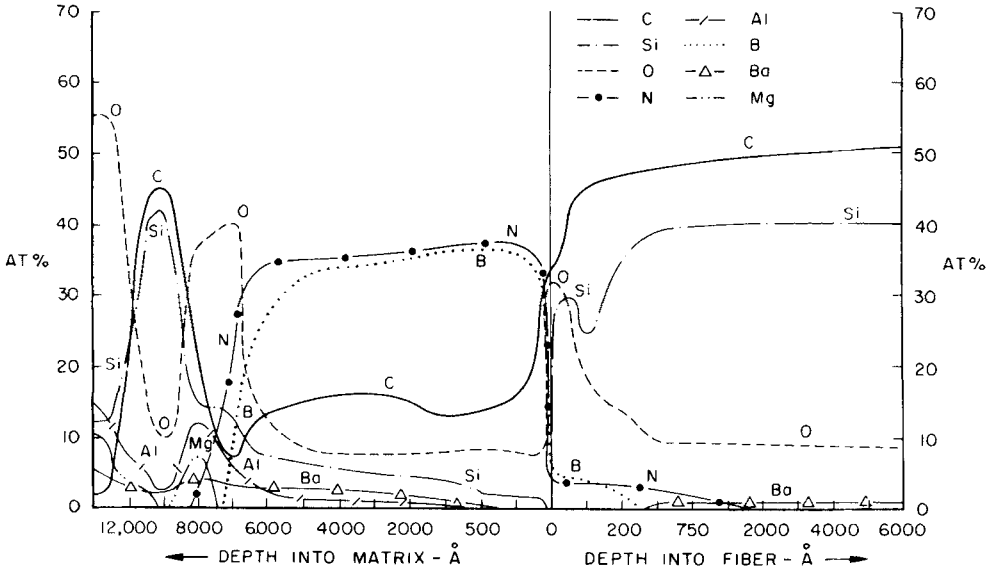

Fig. 3. SAM depth profile of interfacial chemistry in as-pressed composite.

appeared to inhibit diffusion of boron and nitrogen into the adjoining regions of the matrix at this site.

Figure 5 shows a phase-contrast image of the BN/Nicalon fiber interface in the as-pressed composite. A subtle amorphous interlayer, visible as a dual sublayer in Fig. 2, is present between the turbostratic BN layer and the nanocrystalline Nicalon fiber structure. Attempts to use EDS and PEELS to measure the local composition profile of this interface region were inconclusive, possibly because of the extremely small scale of the features (5 to 10 nm) and the lack of sufficient sensitivity to detect differences. However, the AES profile in Fig. 3 shows a layer rich in silica on the fiber side of the debond location, which would correspond to the interlayer shown in Fig. 5. Formation of the interlayer during composite fabrication can occur via a solid-state displacement oxidation reaction, discussed further in Section IV(3).

Matrix element diffusion through the BN layer subsequent to detachment of the SiC layer appeared to contribute to the formation of this interlayer during composite fabrication. Correlation of TEM replicas with thin foil observations and AES data led to the conclusion that both BN coarsening and formation of the carbon–silica interlayer was generally associated with detachment or cracking of the SiC overlayer, followed by glass phase penetration to the BN. Overlayer detachment may be caused by thermally induced stresses that arise from expansion mismatch between the SiC and BN and develop during heating of the composite to the fabrication temperature.

(B) Ceramed Composite: The microstructure of the composite was examined after the ceraming process (1200°C, 24 h, Ar) to determine the effects on the interface. A small amount of residual matrix glassy phase was observed after ceraming, particularly at the interface between the SiC coating and the matrix, as shown in Fig. 6(a). Composition analysis with EDS showed that the glassy phase was enriched in barium and aluminum and apparently depleted in magnesium compared with the crystalline barium osumilite grains. During ceraming, the matrix grains of barium osumilite grew along preferred crystallographic directions in lathlike configurations, often spanning interfiber distances. Ultimately, the grains impinged on obstacles, such as other grains or, more typically, the Nicalon fibers. In Fig. 6(a), three such grains are occluded by a Nicalon fiber. Because of local compositional variations, residual glassy phase often remained at grain boundary interface junctions where the coarse barium osumilite grains terminated.

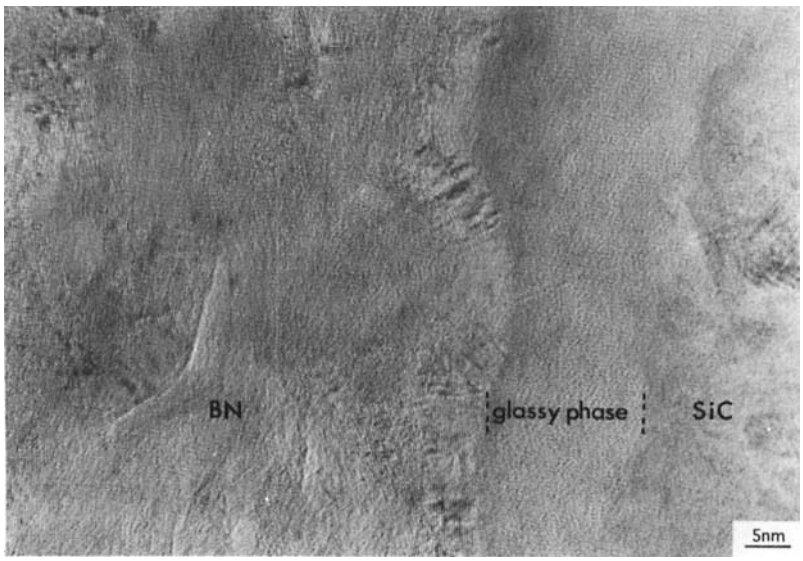

Fig. 4. Amorphous interlayer between the SiC and BN layers in as-pressed composite. The BN layer next to the glassy phase is crystallized.

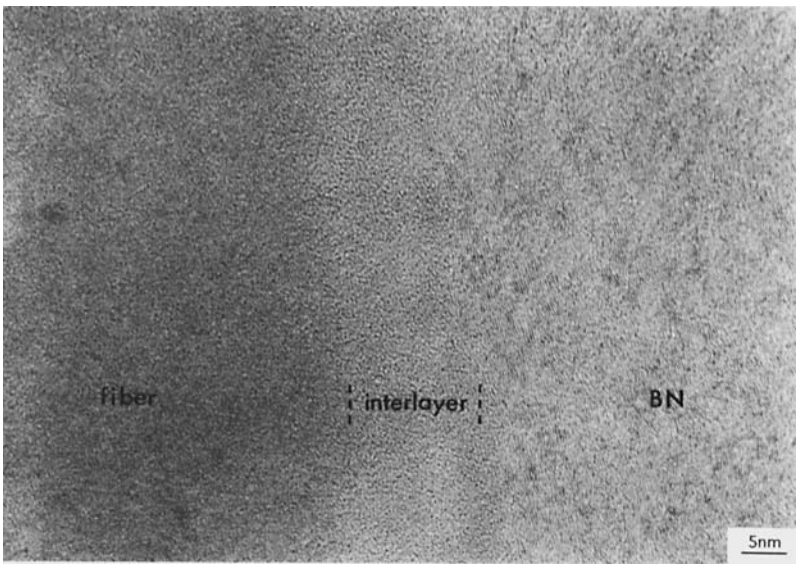

Fig. 5. High-resolution TEM image showing a subtle interlayer region at the BN/Nicalon fiber interface in as-pressed composite.

In addition, intergranular, siliceous glass films, also visible in the image, were often present in the BMAS matrix.

No distinct interlayer was observed at either the SiC/BN interface or the BN/Nicalon fiber interface. An enlarged view of the interface is shown in Fig. 6(b). The image shows a conspicuous absence of the dual sublayers of carbon-rich and silica-rich material between the fiber and the BN coating (cf. Fig. 2).

The SAM depth profile for the ceramed composite is shown in Fig. 7. In this example, the SiC layer remained bonded to the BN layer, thus preventing the penetration of matrix glass. Nevertheless, barium from the matrix diffused through both the SiC layer and BN layers, and into the Nicalon fiber. Barium, despite being a large atom, has consistently been found in this and in previous studies to diffuse relatively rapidly through the SiC and BN layers and deeply into Nicalon fibers. No evidence of carbon or silica film formation at the BN/Nicalon fiber interface was found, which is consistent with the TEM observations in Fig. 6. (The peak in oxygen concentration at the fiber surface is characteristic of the as-received fibers,[5] and the broad oscillation in the carbon profile near the fiber surface does not match with profiles of the carbon-rich interlayer.) Furthermore, matrix elements other than barium did not diffuse to the fiber/matrix interface in this example, a phenomenon that appears to be associated with the adherence of the SiC overlayer, which prevents glass penetration during fabrication.

(C) Interrupted Tensile Stress-Rupture Experiment: A tensile stress-rupture experiment was interrupted prior to failure after ~350 h at 1100°C, having reached a maximum stress level of 165 MPa. However, microscopic observations of the sample revealed microstructural damage in the form of cracks along interfaces and through the matrix. Typical crack paths are shown in Figs. 8(a) and (b) for fiber arrays perpendicular to the direction of applied stress. As shown in the light micrograph of Fig. 8(a), crack propagation occurred through the matrix to the fiber/matrix interface and only in the 90° layers of the 0/90° ply layup composite. The fact that cracks appeared only in the 90° layers, and not in the load-carrying 0° layers, indicates the composite's structural integrity. (Note that failure did *not* occur in this sample.) The TEM micrograph in Fig. 8(b) shows that the crack propagated along the matrix glassy phase that had penetrated between the SiC and BN layers, deflected upward across a barium osumilite grain, and then continued along the matrix/SiC layer interface of another fiber. The matrix grain between the two fibers appears to have sheared where the crack occurred, and dislocations are visible within the grain. These observations indicate that during the test, matrix cracks probably start at a critical flaw in the matrix and propagate to the matrix/fiber interface. Interfacial debonding occurs when the stress at the interface exceeds the interfacial strength, allowing the crack to propagate along the interface.

Cracks propagated most frequently through the BN layer, an example of which is shown in Fig. 9(a). In this case, the crack is between the fine and coarsened BN layer, and appears as a narrow light strip extending diagonally across the image (arrow). Details of the crack are revealed in the high-resolution image in Fig. 9(b), which is an enlargement of the area indicated by the arrow in Fig. 9(a). It is apparent that the opposite surfaces of the crack would fit together if the crack were closed. Figure 9(c) shows the tip area of this particular crack. In this case the crack tip follows the boundary between fine and coarse BN layers. However, crack paths were not always confined to this boundary. Cracking in the fine BN layer and near the BN/Nicalon fiber interface was also observed. Occasionally, debonding occurred in the matrix near the matrix/SiC interface, usually in a layer of residual glass between the SiC layer and a barium osumilite grain.

Two distinct nano-scale sublayers were often observed at the BN/fiber interface in the 90° plies of this composite, as shown in Fig. 9(c). The sublayer on the fiber side is light, while the one on the BN side is dark. Both sublayers are continuous and noncrystalline. The thickness of each sublayer is about 15 nm. The chemistry of the sublayers was determined from EDS composition profiles acquired by stepping the probe across the BN/Nicalon fiber interface (see Tables III and IV). The light sublayer next to the Nicalon fiber was carbon-rich, while the dark sublayer next to the BN was silica-rich. These observations are consistent with previous studies reported by Bonney and Cooper on a Nicalon-fiber-reinforced CAS composite,[18] and by Naslain *et al.* on a chemical-vapor-infiltrated 2D SiC/BN/SiC-fiber composite.[19] No distinct interlayer was observed in the 0° plies, which were parallel to the tensile stress axis in this composite.

(D) Thermally Aged Composite: Thermal aging at 1200°C for 500 h in air caused no significant changes in the Nicalon fibers, the SiC and BN coating, or the BMAS matrix compared with the ceramed composite, although distinct changes were observed at interfaces. Crystallization of the Nicalon fiber was not observed, indicating that the coated fiber was microstructurally stable in the BMAS matrix for long times at 1200°C in air. The SiC and BN coating remained stable and

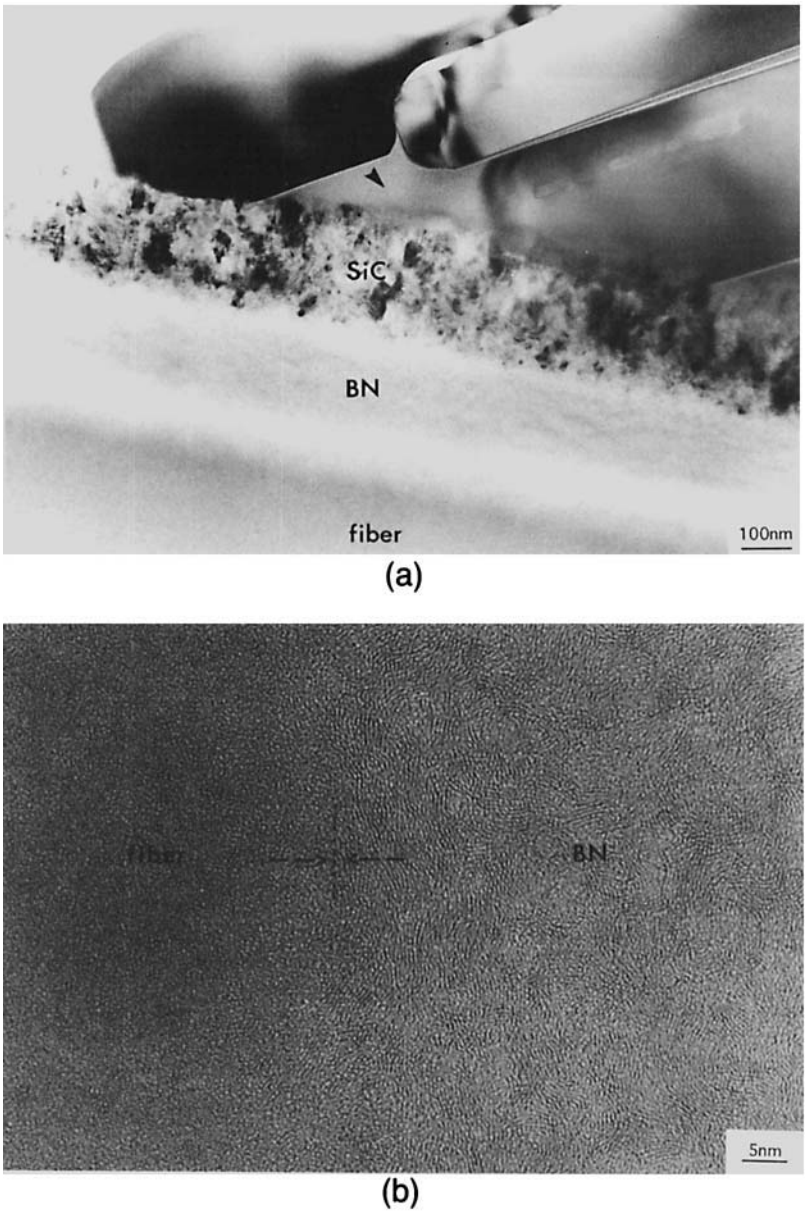

Fig. 6. (a) Residual glassy phase at the matrix/SiC coating interface after ceraming. (b) High-resolution image showing absence of interlayer at the BN/Nicalon fiber interface in ceramed composite.

resistant to both oxidation and gross chemical reaction with the matrix, and the BMAS matrix microstructure did not change.

Various microstructures were observed at the BN/Nicalon fiber interface. Figure 10 shows one interface region in which subtle dual nano-scale sublayers formed at the fiber–coating interface. The SiC coating appears to be well-bonded to the BN layer and no BN coarsening is apparent, implying that matrix elements did not penetrate the SiC overlayer, and that the formation of the dual sublayers does not always occur by oxygen diffusion from the matrix through the BN layer.

In another region of the same sample, pronounced sublayers were observed, as shown in Fig. 11(a). The dark sublayer in this figure is much thicker than in the previous figures. In nearby regions along the same fiber, oxidation reached a more advanced stage, and a gaseous reaction product evolved, creating voids. Figure 11(b) shows voids in the BN layer near the BN/Nicalon fiber interface. The region shown in Fig. 11(a) was the leading edge of an oxidation front that previously passed through the region shown in Fig. 11(b). The voids shown may be formed by the oxidation of carbon present at the fiber surface or contained in the BN layer. (As mentioned in Section III, there is ~20% "excess" carbon in the BN coating.) However, these explanations are speculative, and the exact reaction mechanism presently is not clear.

Compared with composites in as-pressed and ceramed conditions, the microstructure and chemistry at the BN/fiber interface was changed by the thermal aging. The formation of silica-rich and carbon-rich sublayers may be responsible for the observed degradation in the interfacial sliding stress and debond energy, as described in Section IV(1). Lower interfacial sliding stresses and debond energies indicate weaker fiber/matrix bonding. However, the decrease in room-temperature strength of the aged composite is more likely caused by degradation of near-surface fibers.

(3) Formation of the Dual Sublayer Interface

The formation of the dual sublayers is related to diffusion of oxygen and occurs as a result of the displacement reaction:

$$SiC_{(s)} + O_{2(g)} \Rightarrow SiO_{2(s)} + C_{(s)} \quad (1)$$

In addition to Eq. (1), two other equilibria are frequently cited in discussions of oxidation behavior in silicon carbide:

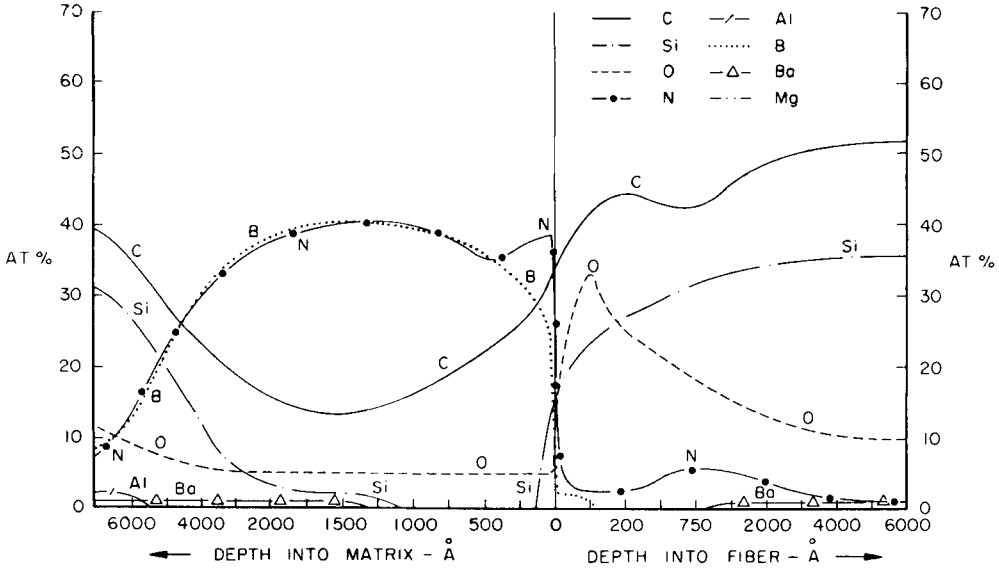

Fig. 7. SAM depth profile of interfacial chemistry in ceramed composite.

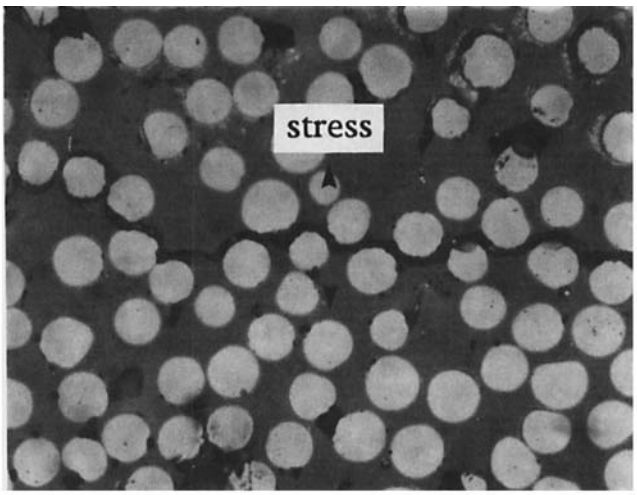

(a)

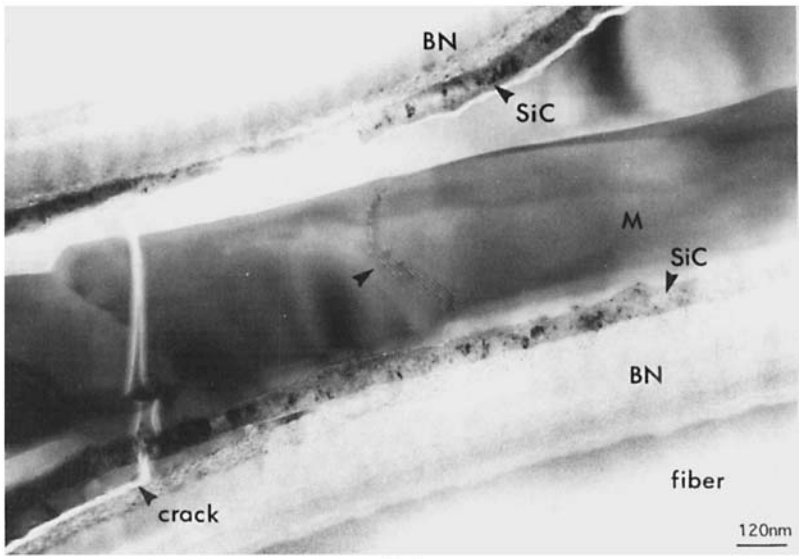

(b)

Fig. 8. Crack propagation in tensile stress-ruptured composite: (a) light micrograph, and (b) TEM micrograph.

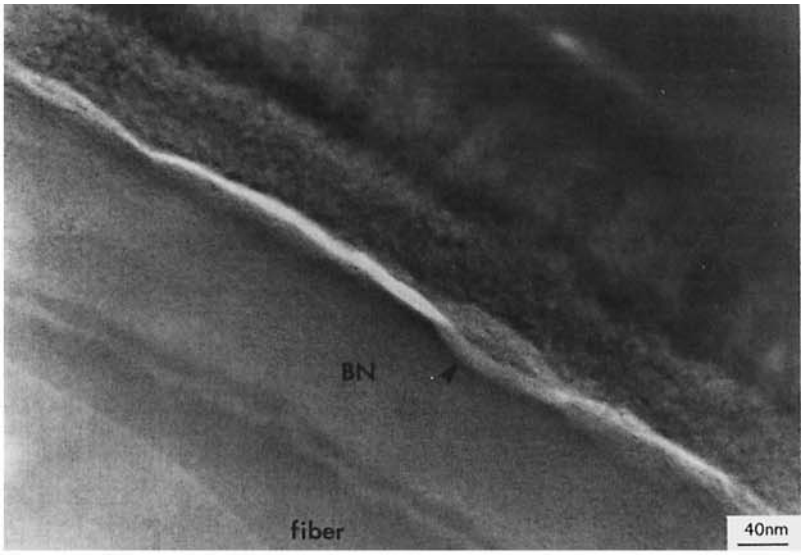

(a)

(b)

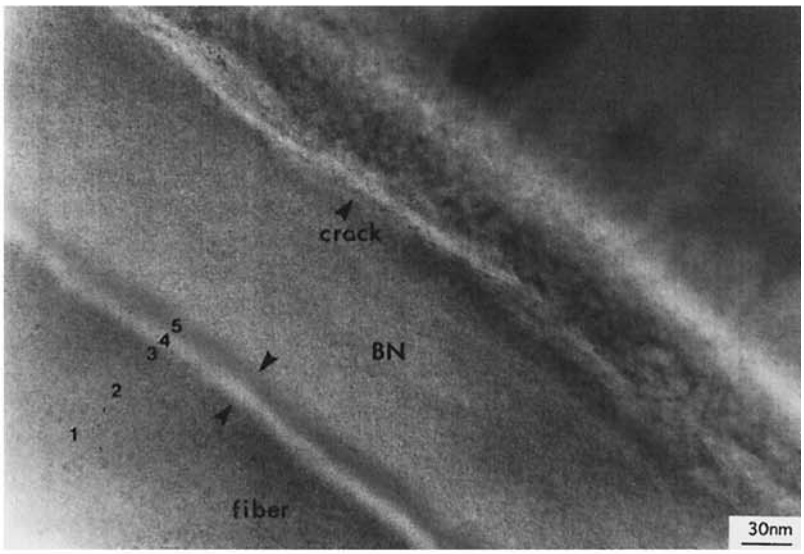

(c)

Fig. 9. (a) Cracking in the BN layer of a 90° fiber after tensile stress-rupture experiment. (b) High-resolution image of the area indicated by arrow in (a). (c) Region near the crack tip.

Table III. Composition Profile (at.%) across the BN/Nicalon Fiber Interface Shown in Fig. 9(c)*

Point	C	O	Si	N
1	43	19	37	
2	43	21	36	
3	41	22	35	
4	39	34	26	
5		48	24	28

*From EDS measurements.

Table IV. Composition Profile (mol%) Calculated from the Data in Table III

Point	Free C	SiC	SiO_2	BN
1	10	59	31	
2	11	55	34	
3	11	53	36	
4	21	21	58	
5			58	42

$$2SiC_{(s)} + 3O_{2(g)} \Rightarrow 2SiO_{2(s)} + 2CO_{(g)} \quad (2)$$

$$SiC_{(s)} + O_{2(g)} \Rightarrow SiO_{2(s)} + CO_{(g)} \quad (3)$$

However, reaction (1) has the most negative free energy change among the three and is likely to exhibit the most rapid reaction kinetics. Thus reaction (1) should dominate the oxidation of Nicalon fibers, provided that the *local* oxygen activity is less than that for reactions (2) and (3). This explanation was proposed by Cooper and Chyung to explain the formation of the carbon-rich interlayer during processing of Nicalon-fiber-reinforced glass and glass-ceramic matrix composites.[4] The morphological aspects of this solid-state displacement reaction were studied in detail by Bonney and Cooper for a Nicalon-fiber-reinforced CAS composite system.[18] They found that in order to form the dual sublayers in a sequence such that the carbon-rich layer is next to the fiber and the silica-rich layer separates the carbon-rich layer from the matrix, the reaction had to be rate-limited by diffusion of oxygen. The oxygen activity in this case is high enough for the displacement reaction to occur and low enough to prevent the volatilization of the carbon-rich layer.

The formation and thickness of the interfacial layer appears to be controlled by the oxygen supply. For composites with uncoated fibers, sources of oxygen are limited to molecular oxygen dissolved in the original glass plus oxygen supplied by heterovalent oxides in the glass that are reduced during consolidation of the composite. However, for coated fibers, there is no direct contact between the matrix and the Nicalon fiber because the coatings act as a diffusion barrier. Even when the SiC layer becomes detached during composite processing, much less oxygen is available at the BN/Nicalon interface compared to uncoated fibers. Thus the reaction is limited, and only a small amount of silica/carbon is produced. As mentioned before, the sublayer in the as-pressed composite is less than 10 nm thick and carbon was not detected by Auger electron spectroscopy. Interestingly, the sublayers, which were sometimes observed by TEM in the as-pressed composites, were rarely observed in composites after the matrix had been crystallized. The explanation for this curious behavior appears to lie in the variability of the coatings. In cases where the SiC overlayer debonded or detached, the glass matrix was able to penetrate to the BN layer and supply sufficient oxygen to the fiber surface for the formation of the sublayers. However, when the SiC overlayer remained intact, the dual sublayers only formed after prolonged exposure to the oxidizing atmosphere, as shown in Fig. 10. In such cases, the oxygen for the reaction at the fiber surface is believed to have been supplied by pipeline diffusion along the fiber interfaces.

Oxygen diffusion from the external environment becomes important during long-term exposure in aerobic environments. This is particularly so when the composite is under stress and oxygen can diffuse along crack openings. For example, in the tensile stress-ruptured composite, the microcracking was perpendicular to the stress axis, i.e., parallel to the 90° fibers, usually in the BN layer, as described previously. Thus more oxygen was able to reach the interface of the fibers, particularly those in the 90° orientation. Consequently, the sublayers were thick and uniform, as shown in Fig. 9(c). In contrast, no distinct interlayer was observed in the 0° plies, as expected, because of the absence of microcracking in these plies. During thermal aging, the dominant oxygen diffusion mechanism is expected to be "pipeline" diffusion. In this process, oxygen supplied from cut surfaces diffuses along the fiber/matrix interfacial region. With sufficient time, oxygen penetrates the composite by diffusion, and the affected zone extends deeper below the surface. This case is illustrated by the 90° fiber shown in Fig. 11. The region in Fig. 11(b) is presumably closer to the supply of oxygen (the composite surface) than the area in Fig. 11(a). If the partial pressure of oxygen in the affected zone is sufficiently high, it is expected to volatilize the carbon present in the BN coating and

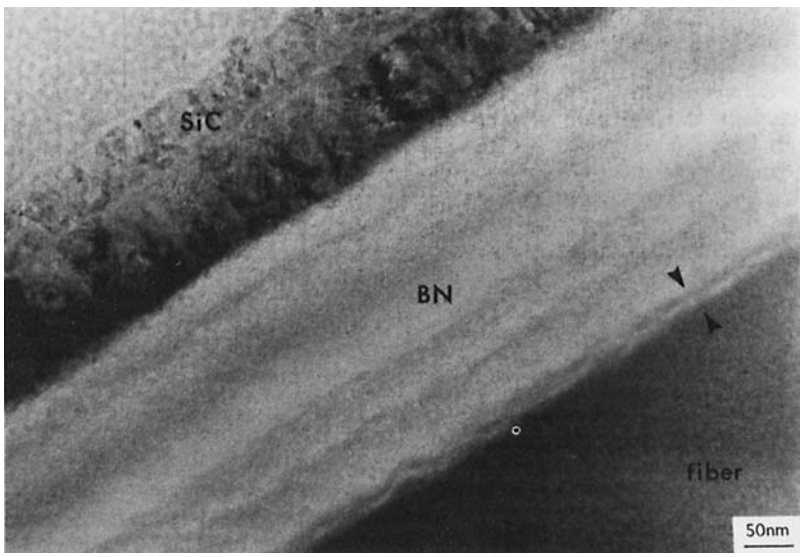

Fig. 10. Interfacial microstructure of thermally aged composite.

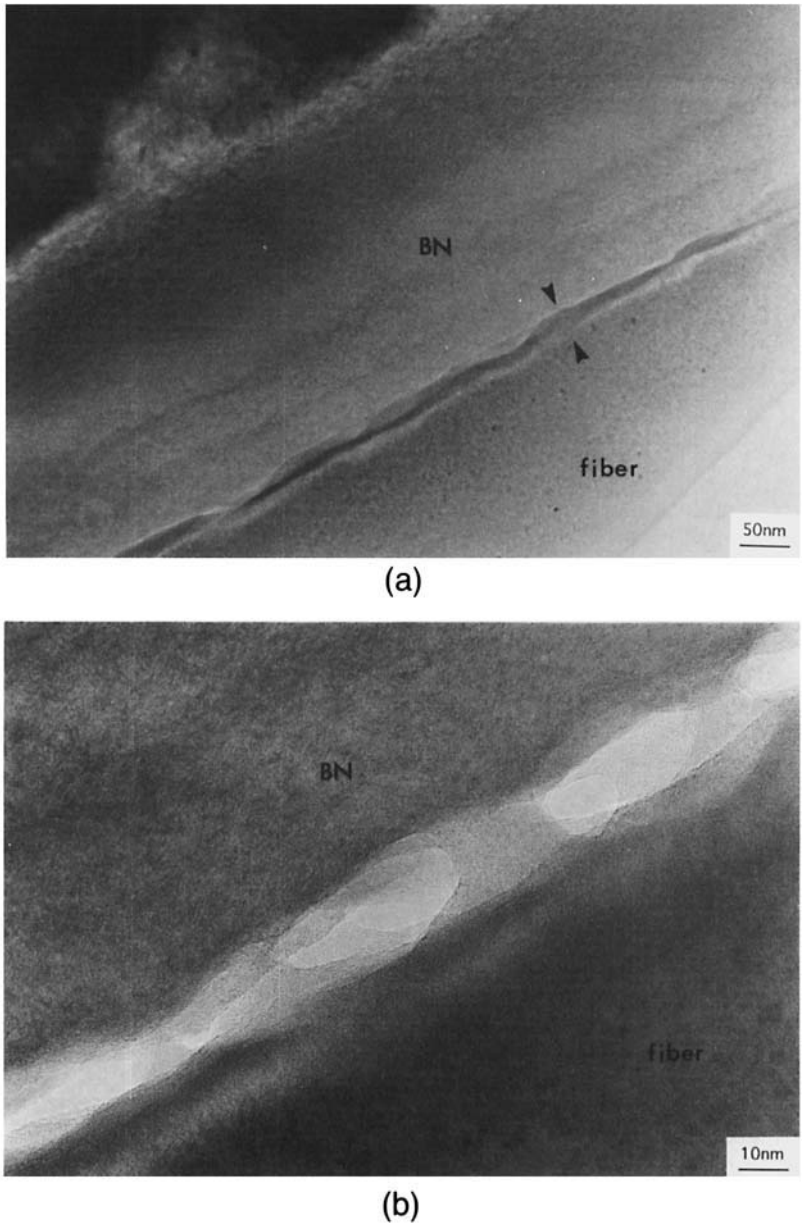

Fig. 11. (a) Interlayers at the BN/Nicalon interface after thermal aging. (b) Affected interfacial zone of the fiber shown in (a).

at the fiber surface, resulting in the formation of gas-filled voids in the BN layer, as shown in Fig. 11(b).

Dual sublayers were observed in the thermally aged composite which was treated at 1200°C for 500 h in air, but not for the 0° fibers in the tensile stress-ruptured composite which was tested for 350 h at 1100°C in air. The diffusion mechanism responsible is presumably the same in both cases, implying that the reaction kinetics for the formation of the sublayer become dominant between ~1100°–1200°C for these time scales.

V. Conclusions

The CVD SiC/BN(C) fiber coatings in the present work hold promise as a viable approach to designing continuous-fiber-reinforced composites. The dual coating functions as a reaction barrier and results in a stable composite microstructure that is resistant to gross chemical reaction during exposure at 1100°C for extended periods of time. The turbostratic BN layer is also a relatively weak interfacial zone, allowing both crack deflection and load transfer to occur so that high fracture toughness is obtained. One problem that remains for the CVD coatings is the frequent debonding of the SiC overlayer from the BN layer, which allows residual glass from the matrix to penetrate and contact the BN layer during consolidation, causing BN coarsening and accelerating the decomposition of the fiber. It is important that the issue of detachment be addressed. One approach currently under investigation involves altering the relative thicknesses of the coatings to reduce the mismatch stress, while retaining the function of a reaction barrier and providing a relatively weak interface.

During long-term exposure to oxygen at high temperature, nano-scale silica/carbon sublayers were formed at the BN/Nicalon fiber interface. These sublayers may be responsible for the decrease in the fiber/matrix bonding strength. There appears to be a temperature range between 1100° and 1200°C, below which the reaction kinetics for the formation of the sublayers are sufficiently slow that the sublayers do not form for long periods of time. Consequently, the interfacial properties and the composite mechanical properties are expected to be maintained after thermal aging at 1100°C for extended periods. Thus, this particular composite system offers excellent potential as a tough and thermally stable structural material for high-temperature applications.

Acknowledgments: We would like to thank Mr. Jim O'Kelly of 3M for coating the Nicalon fibers used in the study, Dr. Bruce Laube and Mr. Dan Delong of UTRC for the SAM analyses, Mr. Stan Kustra of UTRC and Mr. Gary Linsey of Pratt & Whitney for the composite mechanical testing, Dr. Paul Jero at Wright-Patterson AFB for fiber indent testing, and Lt. Col. Alexander Pechenik of AFOSR for sponsorship of this program.

References

[1]K. M. Prewo and J. J. Brennan, "High Strength Silicon Carbide Fiber-Reinforced Glass Matrix Composites," *J. Mater. Sci.*, **15,** 463–68 (1980).

[2]K. M. Prewo and J. J. Brennan, "Silicon Carbide Fiber Reinforced Glass-Ceramic Matrix Composites Exhibiting High Strength and Toughness," *J. Mater. Sci.*, **17,** 2371–83 (1982).

[3]J. J. Brennan, "Interfacial Characterization of Glass and Glass-Ceramic Matrix/Nicalon SiC Fiber Composites"; pp. 549–60 in *Materials Science Research*, Vol. 20. Plenum Press, New York, 1986.

[4]R. F. Cooper and K. Chyung, "Structure and Chemistry of Fiber–Matrix Interfaces in SiC Fibre-Reinforced Glass-Ceramic Composites: An Electron Microscopy Study," *J. Mater. Sci.*, **22,** 3148–60 (1987).

[5]J. J. Brennan, "Glass and Glass-Ceramic Matrix Composites"; Ch. 8 in *Fiber Reinforced Ceramic Composites*. Edited by K. S. Mazdiyasni. Noyes, Park Ridge, NJ, 1990.

[6]R. W. Rice, "BN Coating of Ceramic Fibers for Ceramic Fiber Composites," U.S. Pat. No. 4 642 271, February 10, 1987.

[7]R. N. Singh, "Fiber-Matrix Interfacial Characteristics in a Fibre-Reinforced Glass-Ceramic Composites," *J. Am. Ceram. Soc.*, **72** [9] 1764–67 (1989).

[8]W. K. Tredway and K. M. Prewo, "Improved Performance in Monofilament Fiber Reinforced Glass Matrix Composites Through the Use of Fiber Coatings," *Mater. Res. Soc. Symp. Proc.*, **170,** 215–21 (1990).

[9]J. J. Brennan, "Interfacial Studies of Coated Fiber Reinforced Glass-Ceramic Matrix Composites," Annual Rept. No. R90-918185-2 on AFOSR Contract No. F49620-88-C-0062, September 30, 1991.

[10]J. J. Brennan, B. Allen, S. R. Nutt, and Y. Sun, "Interfacial Studies of Coated Fiber Reinforced Glass-Ceramic Matrix Composites," Annual Rept. No. R92-970150-1 on AFOSR Contract No. F49620-92-C-0002, November 30, 1992.

[11]K. M. Prewo, J. J. Brennan, and G. K. Layden, "Fiber Reinforced Glasses and Glass-Ceramics for High Performance Applications," *Am. Ceram. Soc. Bull.*, **65** [2] 305–13, 322 (1986).

[12]D. B. Marshall, "An Indentation Method for Measuring Matrix/Fiber Frictional Stresses in Ceramic Composites," *J. Am. Ceram. Soc.*, **67** [12] C-259–C-260 (1984).

[13]D. B. Marshall and W. C. Oliver, "Measurement of Interfacial Mechanical Properties in Fiber-Reinforced Ceramic Composites," *J. Am. Ceram. Soc.*, **74** [3] 542–48 (1987).

[14]P. Schreck, C. Vix-Guterl, P. Ehrburger, and J. Lahaye, "Reactivity and Molecular Structure of Silicon Carbide Fibers Derived from Polycarbosilanes," *J. Mater. Sci.*, **27,** 4237–42 (1992).

[15]C. Laffon, A. M. Flank, P. Lagarde, M. Laridjani, R. Hagege, P. Olry, J. Cotteret, J. Dixmier, J. L. Miquel, H. Hommel, and A. P. Legrand, "Study of Nicalon-Based Ceramic Fibres and Powders by EXAFS Spectrometry, X-Ray Diffractometry and Some Additional Methods," *J. Mater. Sci.*, **24,** 1503 (1989).

[16]F. Saygnac, F. Teyssandier, and A. Marchand, "Characterization of C-B-N Solid Solutions Deposited from a Gaseous Phase Between 900° and 1050°C," *J. Am. Ceram. Soc.*, **75** [1] 161–69 (1992).

[17]T. T. Borek, X. Qiu, L. M. Rayfuse, A. K. Datye, and R. T. Paine, "Boron Nitride Coatings on Oxide Substrates: Role of Surface Modifications," *J. Am. Ceram. Soc.*, **74** [10] 2587–91 (1991).

[18]L. A. Bonney and R. F. Cooper, "Reaction-Layer Interfaces in SiC-Fiber-Reinforced Glass-Ceramics: A High-Resolution Scanning Transmission Electron Microscopy Analysis," *J. Am. Ceram. Soc.*, **73** [10] 2916–21 (1990).

[19]R. Naslain, O. Dugne, A. Guette, J. Sevely, C. R. Brosse, J.-P. Rocher, and J. Cotteret, "Boron Nitride Interphase in Ceramic-Matrix Composites," *J. Am. Ceram. Soc.*, **74** [10] 2482–88 (1991). □